DØ note # 3231
May 18, 1998
Draft v3.2

Mining Gold in $\gamma \not\!\!E_T + n$ Jets Final States

Sailesh Chopra, Jianming Qian

Department of Physics, The University of Michigan
Ann Arbor, Michigan 48109

We search for excesses of $\gamma \not\!\!E_T$ events with two or more jets in $p\bar{p}$ collisions at $\sqrt{s} = 1.8$ TeV for new physics. Such events are expected from production of supersymmetric particles. No excess of events beyond the expected background is observed. For the region of the MSSM parameter space with $\mathrm{Br}(\tilde{\chi}_2^0 \to \tilde{\chi}_1^0 \gamma) = 100\%$ and $m_{\tilde{\chi}_2^0} - m_{\tilde{\chi}_1^0} > 20$ GeV/c^2, we obtain a 95% CL lower mass limit of 311 GeV/c^2 for squarks and gluinos assuming equal squark and gluino mass. In short, no gold was found. Instead we found that our limit is stronger and more general than CDF's limit derived from their $\gamma b \not\!\!E_T$ analysis.

I. INTRODUCTION

Events with a high E_T photon, multi-jets and large missing transverse energy ($\not\!\!E_T$) are predicted in supersymmetric extensions of the Standard Model. Supersymmetry [1] is a generalization of space-time symmetry. It predicts that elementary particles come in Boson-Fermion pairs. The minimal supersymmetric standard model (MSSM) is realized by adding a second higgs doublet and supersymmetrizing the gauge theory of the standard model. In the framework of MSSM, the gaugino-higgsino sector (excluding the gluino) is described by four parameters, M_1, M_2, μ and $\tan\beta$, where M_1 and M_2 are the $U(1)$ and $SU(2)$ gaugino mass parameters at the electroweak scale, μ is the higgsino mass parameters and $\tan\beta$ is the ratio of the vacuum expectation values of the two higgs doublets. As a result of the electroweak symmetry breaking, gauginos and higgsinos mix to form four neutral mass eigenstates (neutralinos) and two charged mass eigenstates (charginos). They are denoted by $\tilde{\chi}_i^0, i = 1, 2, 3, 4$ and $\tilde{\chi}_j^{\pm}, j = 1, 2$.

Recently in an effort to explain a CDF event [2], it has been suggested [3] that $\tilde{\chi}_1^0$ and $\tilde{\chi}_2^0$ are dominated by higgsino and gaugino components respectively. In this scenario, the radiative decay of $\tilde{\chi}_2^0 \to \tilde{\chi}_1^0\gamma$ is enhanced. Detailed analysis [4] of the supersymmetric parameter space shows that this can be achieved when the supersymmetric parameters take the following values: $50 \lesssim M_1 \sim M_2 \lesssim 100$ GeV, $1 \lesssim \tan\beta \lesssim 3$ and $-65 \lesssim \mu \lesssim -35$ GeV *. In addition, the rate and kinematics of the event imply

$$\mathrm{Br}(\tilde{\chi}_2^0 \to \tilde{\chi}_1^0\gamma) \sim 100\%$$

$$m_{\tilde{\chi}_2^0} - m_{\tilde{\chi}_1^0} \gtrsim 20 \text{ GeV/c}^2.$$

The often-assumed gaugino mass unification is not satisfied by these models. Assuming $\tilde{\chi}_1^0$ is the lightest supersymmetric particle (LSP) and R-parity [5] is conserved, the $\tilde{\chi}_1^0$ is stable and weakly-interacting. The production of squarks ($\tilde{q}$) and gluinos ($\tilde{g}$) with their subsequent direct or cascade decays to $\tilde{\chi}_2^0$ will result in events with a high E_T photon, multi-jets and large $\not\!\!E_T$. For convenience, the events with a high E_T photon, large $\not\!\!E_T$ and n or more jets are called $\gamma\not\!\!E_T + \geq n$ jets events.

We have reported a search for $\gamma\gamma\not\!\!E_T$ events as predicted by supersymmetric models with a light gravitino in [6]. In this note, we present the first experimental search for excess of $\gamma\not\!\!E_T$ events with two or more jets in $\sqrt{s} = 1.8$ TeV $p\bar{p}$ collisions at the Fermilab Tevatron. Theoretically, the $\gamma\not\!\!E_T + \geq n$ jets final state is attractive since there is little backgrounds from Standard Model processes at parton level [7]. Unfortunately, there are large instrumental backgrounds. We compare the observed event rates with the expectations from known sources. The implications of this analysis for supersymmetric models are discussed. Despite the theoretical interest, so far there are no published experimental data on this final state. Although motivated by supersymmetric models, our goal is to study the $\gamma\not\!\!E_T + \geq n$ jets

---

*Is this type of models crazy? Yes, it is as crazy as all other model (supergravity, leptoquark, compositeness... you name it.) Do we believe it? No. However we are open minded. God didn't consult us when the world was created. History has shown that God does play dice...

event topology for new physics. The results of the analysis can be applied to other new physics models with similar topologies, such as supersymmetric models with a light gravitino and a long lived $\tilde{\chi}_1^0$ [8]. Due to the large backgrounds from QCD multijet and W+jets production, $\gamma \not\!\!E_T$ events with less than two jets are not considered in this analysis.

The data used in this analysis were collected with the DØ detector during the 1992-1996 Tevatron runs (Run 1A, 1B and 1C) at $\sqrt{s} = 1.8$ TeV. Runs with Main Ring active were vetoed using the MRBS_LOSS and MICROBLANK for Run 1B and 1C and only the MICROBLANK for Run 1A. The total effective luminosity used in this analysis is $99.4 \pm 5.4\,\mathrm{pb}^{-1}$. The DØ detector consists of a non-magnetic central tracking system, a calorimeter, and a toroidal muon spectrometer. With the hermetic and uniform rapidity coverage of the calorimeter, the DØ detector is well suited for searching for new physics with large missing transverse energy. A detailed description of the DØ detector can be found in Ref. [9].

The rest of the note is organized as following. We briefly review the event reconstruction, followed by the detailed presentations of event selections, background estimations and finally the limits on supersymmetric models.

II. EVENT RECONSTRUCTION

Photons are identified by the detection of an isolated electromagnetic (EM) cluster in the calorimeter and by the absence of a track and the absence of a large number of hits in the tracking chamber in roads between the calorimeter shower and the event vertex. The identification procedure is briefly reviewed below. Details can be found in Ref. [6].

The EM clusters are selected from calorimeter energy clusters by requiring

(1) at least 95% of the energy to be deposited in the EM section of the calorimeter,

(2) the transverse and longitudinal shower profiles to be consistent with those expected for an EM shower ($\chi^2 < 100$), and

(3) the energy in an annular isolation cone from radius 0.2 to 0.4 around the cluster in $\eta - \phi$ space to be less than 10% of the cluster energy, where η and ϕ are the pseudorapidity and azimuthal angle.

The efficiency (ϵ_C) of the these selection criteria on reconstructed PELC/PPHO's with $E_T > 20$ GeV is estimated using ELE triggers. It is found that the efficiency varies slightly with the minimum number of jets in an event. Table I shows ϵ_C's for events with at least 0, 1 and 2 jets for CC ($|\eta| < 1.2$) and EC ($1.5 < |\eta| < 2.0$) separately. As the jet activity is increased, the efficiency decreases slightly for CC and is constant within the statistics for EC. Therefore, for the analysis described below, we use $\epsilon_C = 0.845 \pm 0.039$ for CC and $\epsilon_C = 0.848 \pm 0.027$ for EC.

Photons are further selected from the identified EM clusters using the tracking information by requiring that there should be no reconstructed track nor a large number of hits in the tracking chamber in angular roads (calculated using HITSINFO package) between the calorimeter cluster and the event vertex. The efficiency of the HITSINFO requirement is estimated using the $Z \to ee$ data events which are selected from events passing the Level 2 filter EM2_EIS2HI. To increase statistics, a loose electron identification ($\chi^2 < 200$ and isolation

# of jets	CC	EC
$n \geq 0$	0.918±0.027	0.848±0.027
$n \geq 1$	0.902±0.040	0.848±0.033
$n \geq 2$	0.845±0.039	0.896±0.078

TABLE I. Efficiencies of photon identification selection as functions of the minimum number of jets.

$\mathcal{I} < 0.15$) is applied. In addition, electrons are required to have $E_T > 20$ GeV and $|\eta| < 2.0$. Moreover, the invariant mass of the electron pair must be within the ± 5 GeV/c^2 window around M_Z.

To estimate the HITSINFO selection efficiency, the calorimeter clusters of the electrons are rotated by an angle $\pi/2$ in the $r - \phi$ plane. Since a rotated cluster could overlap with a real jet, the calorimeter energy in the neighboring cells of the rotated cluster direction is required to be less than 4 GeV. Two new roads are then constructed between the rotated cluster and the event vertex. The first one is a wide road (called PPHO road) and the second one is a narrow road (called HITSINFO road). All HITSINFO variables are computed using the new HITSINFO road. The HITSINFO efficiency is then the fraction of the rotated clusters with no reconstructed tracks in the PPHO road and passing the HITSINFO requirement. Since the data $Z \to ee$ events are used, the efficiency is automatically luminosity weighted and takes into account effects such as track overlaps from underlying events and detector noises.

The efficiencies for events with different numbers of jets are summarized in Table II, where jets are required to have $E_T > 20$ GeV and $|\eta| < 2.0$. Though the efficiency decreases slightly as the number of jets increases, they agree within errors. For this analysis, the HITSINFO efficiencies of $\epsilon_H = 0.759 \pm 0.040$ for CC and $\epsilon_H = 0.776 \pm 0.060$ for EC are used.

Number of	Efficiencies (%)		
jets	CC	EC	CC+EC
≥ 0	79.1±1.2	79.2±2.1	79.2±1.0
≥ 1	77.1±2.1	78.2±3.6	77.4±1.9
≥ 2	75.9±4.0	77.6±6.0	76.4±3.3
≥ 3	75.0±8.3	80.9±9.5	77.2±5.6

TABLE II. HITSINFO efficiencies for events with different numbers of jets for CC, EC and CC/EC combined.

However, the ϵ_H determined above does not include the effect of photon conversions in materials in front of the tracking chamber. The probability (ϵ_X) for non-conversion is determined from the fully simulated single photon events to be 0.90 ± 0.01 for CC photons and 0.70 ± 0.03 for EC photons.

The total efficiency ($\epsilon_\gamma = \epsilon_C \times \epsilon_H \times \epsilon_X$) [†] for identifying a $E_T > 20$ GeV photon after being reconstructed as a PPHO object is $\epsilon_\gamma = 0.58 \pm 0.04$ for CC and $\epsilon_\gamma = 0.46 \pm 0.04$ for EC.

Due to the imperfect tracking detector and tracking algorithm, an electromagnetic cluster produced by an electron can be misidentified as a photon. To aid the background estimation, we introduce an electron rejection factor (R) which is defined as the ratio between the numbers of electrons and photons identified from a sample of electron–originated electromagnetic clusters. Unless otherwise specified, electrons are selected from PELC objects and must pass the criteria for the electromagnetic clusters and have track–match significances ($\sigma_{\rm TM}$) less than 5. The rejection is calculated using the same method described in Ref. [11]. It consists of two components: rejection provided by the track (by only considering PPHO objects as photon candidates) and the rejection provided by the HITSINFO selection.

The rejection from the track (R_T) is calculated using the tracking finding efficiency (ϵ_t) and the efficiency (ϵ_m) for track–match significance requirement reported in [10] using the formula:

$$R_T = \frac{\epsilon_t \epsilon_m}{1 - \epsilon_t}.$$

It is found to be 6.1 ± 0.3 for CC and 4.7 ± 0.2 for EC for the efficiencies ($\epsilon_t = 0.864 \pm 0.014$, $\epsilon_m = 0.934 \pm 0.009$ for CC and $\epsilon_t = 0.861 \pm 0.018$, $\epsilon_m = 0.766 \pm 0.028$ for EC) presented in [10]. The rejection of the HITSINFO selection in DØRECO version 12.20 or higher is estimated using the loose $W \rightarrow$'e'ν events. This sample is selected by requiring one PPHO cluster passing the electromagnetic identification and with $E_T > 20$ GeV. In addition, the events are required to have $\not\!\!E_T > 25$ GeV. The HITSINFO selection is then applied to the sample. After subtracting QCD backgrounds from the sample both before and after HITSINFO selection, rejection factors (R_H) of 37.5 ± 5.9 for CC and 35.9 ± 8.4 for EC are obtained. Combining the rejections of the track and the HITSINFO selection, the tracking provided a total electron rejection factor ($R = R_H \times R_T$) of 229 ± 38 for CC and 169 ± 37 for EC. These numbers are in good agreement with 245 ± 60 for CC and 160 ± 50 for EC reported in [11] for Run 1A. The HITSINFO selection in DØRECO versions earlier than 12.20 is found to be inefficient in reducing backgrounds for photons.

The validity of the HITSINFO rejection of electrons is checked using a sample of $Z \rightarrow ee$ events, which are selected by requiring two electromagnetic clusters each with $E_T > 20$ GeV and an invariant mass of the pair $86 < M_{ee} < 96$ GeV/c^2. The electromagnetic cluster can either be a PELC or a PPHO object. The HITSINFO rejection is then obtained by imposing the selection to the PPHO clusters. The rejection factor obtained for the CC is 40 ± 7, in agreement with that estimated using the loose W events.

The probability ($\mathcal{P}_{j \rightarrow \gamma}$) for misidentifying a jet as a photon was measured to be $(7 \pm 2) \times 10^{-4}$ [12] by counting the number of photons in multijet events.

[†]This calculation ignores the contribution due to converted photons. For a converted photon to be identified as a photon, it has to have no track reconstructed and no random overlap track in the road and to pass the HITSINFO selection. The contribution to the efficiency due to converted photons is estimated to be less than 0.2%.

Jets are reconstructed using a cone algorithm with radius $\mathcal{R} \equiv \sqrt{(\Delta\phi)^2 + (\Delta\eta)^2} = 0.5$ in $\eta - \phi$ space. The jet energy scale is determined by demanding the transverse energy balance in direct photon events.

The missing transverse energy is calculated from energy deposits in individual calorimeter cells having $|\eta| < 4.5$ using the vertex position determined by the tracking chambers and is defined to be the negative of the vector sum of the cell transverse energies.

III. SEARCH FOR $\gamma \not\!\!E_T + \geq n$ jets EVENTS

This analysis is restricted to events from the Level 2 filter ELE_JET for Run 1A and ELE_JET_HIGH for Run 1B/1C. The ELE_JET filter requires one EM cluster with $E_T >$ 15 GeV, one jet with $E_T > 10$ GeV, and $\not\!\!E_T >$ 10 GeV. Apart from the $\not\!\!E_T$ requirement for which the threshold is raised to 14 GeV, the other requirements for the ELE_JET_HIGH filter are identical to those of the ELE_JET filter.

A. Event Selection

The $\gamma \not\!\!E_T + \geq n$ jets candidate events are selected through a two-step processes, necessitated by the fact that not all of the data were reconstructed with the reliable HITSINFO package [‡].

Firstly, a looser photon identification without the HITSINFO requirement but including all other requirements is used to select a loose sample of $\gamma + \geq 2$ jets events which have one loose photon ($E_T^\gamma > 20$ GeV, $|\eta^\gamma| < 1.2$ or $1.5 < |\eta^\gamma| < 2.0$) and two or more jets ($E_T^j > 20$ GeV, $|\eta^j| < 2.0$). The $\not\!\!E_T$ distribution of the selected events from Run 1B/1C is shown in Fig. 1. Also shown is the expected distribution from the QCD background discussed below.

Secondly, 6013 $\gamma + \geq 2$ jets events with $\not\!\!E_T >$ 25 GeV are picked using the PICK_EVENTS utility and reprocessed with the CAFIX version 5.1 and the good HITSINFO packages. After applying the HITSINFO requirement to the reprocessed events, 318 events ($\gamma \not\!\!E_T + \geq 2$ jets) remain in the sample [§]. Seventy of these events have three or more jets ($\gamma \not\!\!E_T + \geq 3$ jets) and 8 have four or more jets ($\gamma \not\!\!E_T + \geq 4$ jets). This set of the selection criteria is called basic selection and the $\gamma \not\!\!E_T + \geq 2$ jets sample is referred as the base sample for convenience.

The azimuthal angle distribution of the $\not\!\!E_T$ of the 318 $\gamma \not\!\!E_T + \geq 2$ jets events is shown in Fig. 2. The distribution is essentially flat implying that the main ring does not seem to be a problem. The kinematic distributions of the base sample are compared with the expected distributions from backgrounds (see next section) in Fig. 3 for the photon E_T, Fig. 4 for the

---

[‡]Only $\sim$ 15% of the data were processed with DØRECO version 12.20 or higher, which has a valid HITSINFO package.

[§]The number of events surviving the HITSINFO cut would be 378 if they were not reprocessed with CAFIX 5.1.

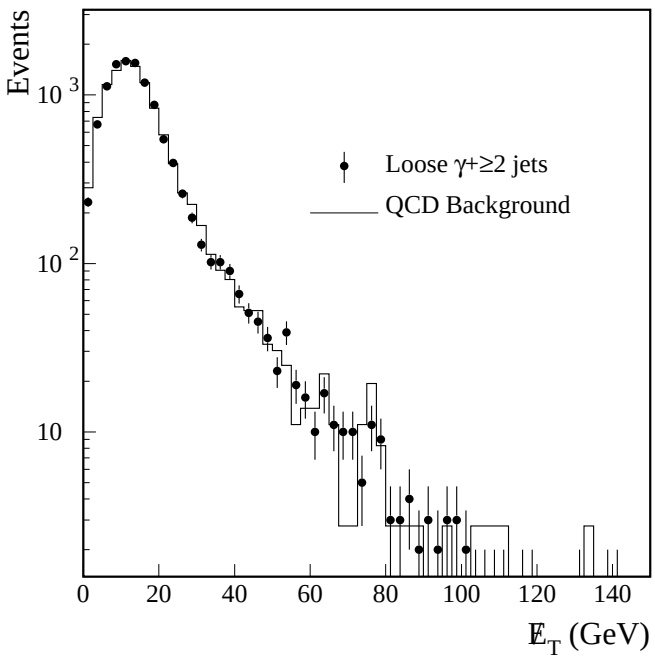

FIG. 1. The $\not\!\!E_T$ distribution of the loose $\gamma+ \geq 2$ jets events (from Run 1B/1C) compared with the expectation from the QCD events. The two distributions are normalized to have equal entries. The apparent good agreement between the two distributions implies that the measured $\not\!\!E_T$ of the loose $\gamma+ \geq 2$ jets events is largely due to mismeasurement.

jet multiplicity, Fig. 5 for the E_T of the leading jet, Fig. 6 for the E_T of all jets, and in Fig. 7 for the four $r-\phi$ opening angles. Most of these events have two jets and soft E_T spectra for photons and jets. As shown in Fig. 7(b), the $\not\!\!E_T$ direction in $r-\phi$ is strongly correlated with that of the leading jet, implying that the $\not\!\!E_T$ mismeasurement is a main background source.

B. Background Estimation

Though there is no significant physics background for the $\gamma\not\!\!E_T+ \geq n$ jets final states, there are important instrumental backgrounds. Multijet, direct photon, $W(\rightarrow \ell\nu)$+jets, $Z(\rightarrow \nu\nu)$+jets from the Standard Model processes with misidentified photons and/or mismeasured $\not\!\!E_T$ are the principal background sources. The numbers of background events from these sources are estimated using data separately for the following three cases:

(1) QCD Background: $\gamma+ \geq 2$ jets (real or fake γ) events without genuine $\not\!\!E_T$ would fake $\gamma\not\!\!E_T+ \geq n$ jets events if $\not\!\!E_T$'s are significantly mismeasured.

(2) e+jets background: $W(\rightarrow e\nu)$+jets events would be misidentified as $\gamma\not\!\!E_T+ \geq n$ jets events if the electrons are misidentified as photons.

(3) ν+jets background: $W(\rightarrow \ell\nu)$+jets and $Z(\rightarrow \nu\nu)$+jets events would be selected as $\gamma\not\!\!E_T+ \geq n$ jets events if one of the jets in the events is misidentified as a photon.

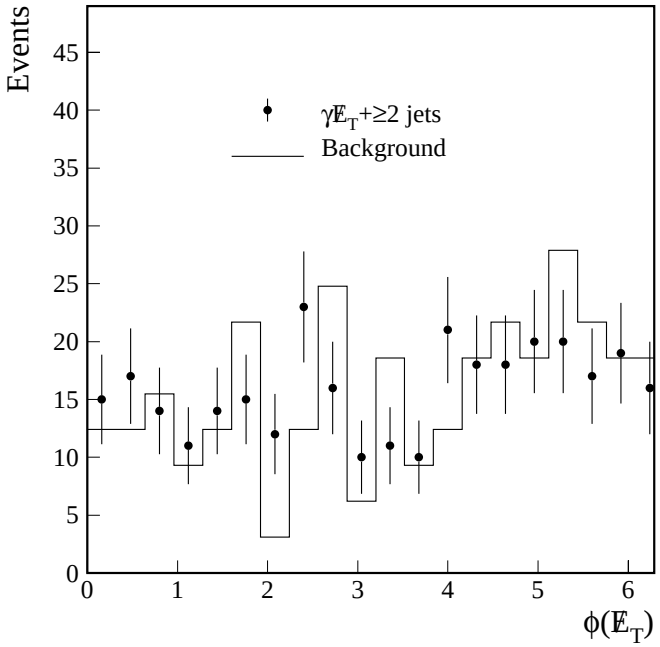

FIG. 2. The azimuthal angle distribution of the $\not\!\!E_T$ of the $\gamma+ \geq 2$ jets events. Also shown is the distribution expected from the background events. The two distributions agree well and are essentially flat. A horizontal line fit yields χ^2/n.d.f. of 18/19 for the data and 23/19 for the background. The main ring activity is not problem for this analysis.

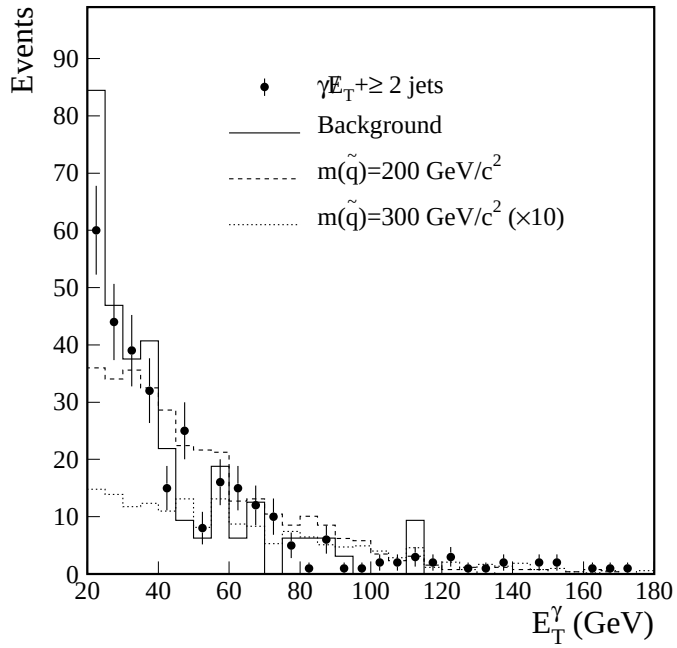

FIG. 3. Photon E_T distributions of the 318 $\gamma\not\!\!E_T$ events with two or more jets and of the background events. Also shown are the expected distributions (multiplied by 10 for the case $m_{\tilde{q}} = 300$ GeV/c^2) from supersymmetry for two different values of squark/gluino masses. The numbers of events expected are 324 for $m_{\tilde{q}} = 200$ GeV/c^2 and 17.3 for $m_{\tilde{q}} = 300$ GeV/c^2.

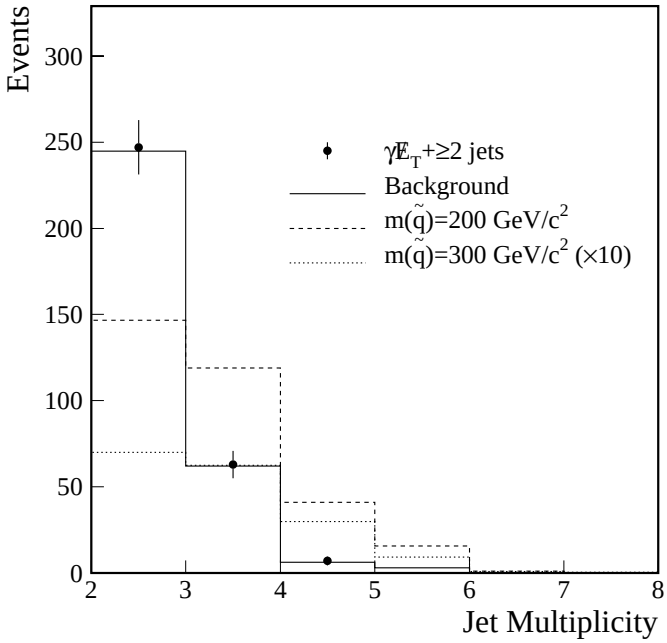

FIG. 4. The jet multiplicity distributions of the $\gamma \not\!\!E_T + \geq 2$ jets and background events. Also shown are the expected distributions (multiplied by 10 for the case $m_{\tilde{q}} = 300$ GeV/c^2) from supersymmetry for two different values of squark/gluino masses assuming an equal squark and gluino mass.

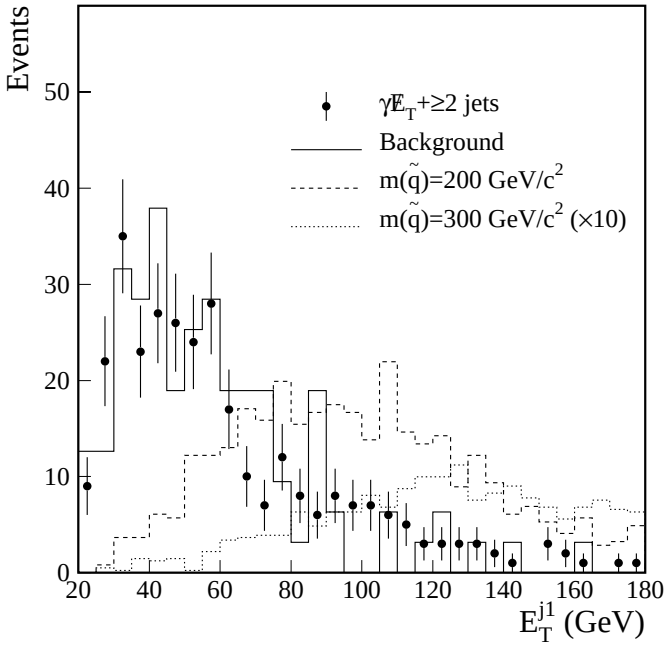

FIG. 5. The leading jet E_T distributions of the $\gamma \not\!\!E_T + \geq 2$ jets and background events. Also shown are the expected distributions (multiplied by 10 for the case $m_{\tilde{q}} = 300$ GeV/c^2) from supersymmetry for two different values of squark/gluino masses assuming an equal squark and gluino mass.

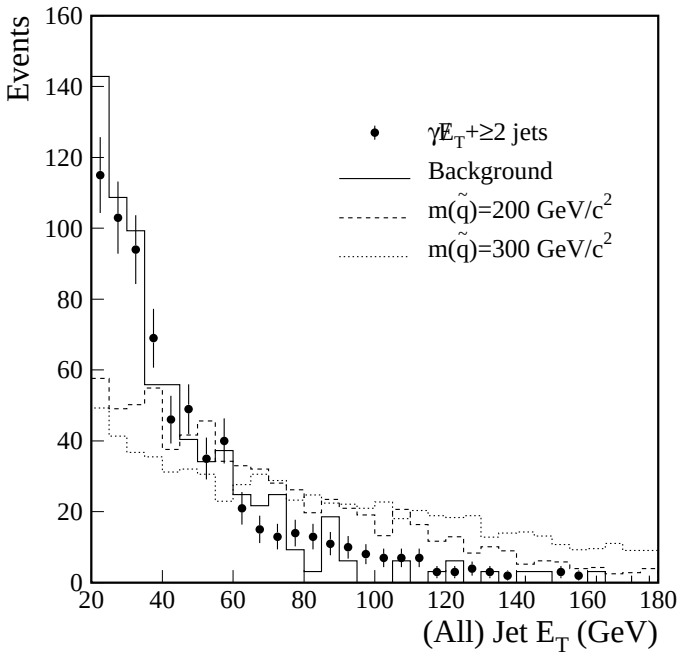

FIG. 6. The (all) jet E_T distributions of the $\gamma\not\!\!E_T+ \geq 2$ jets and background events. Note that all distributions are normalized to equal entries. Also shown are the expected distributions (multiplied by 10 for the case $m_{\tilde{q}} = 300$ GeV/c^2) from supersymmetry for two different values of squark/gluino masses assuming an equal squark and gluino mass.

1. QCD Background

The QCD background is estimated using a sample of events with one EM-like cluster ($E_T > 20$ GeV, $|\eta| < 1.2$ or $1.5 < |\eta| < 2.0$) and two or more jets ($E_T > 20$ GeV, $|\eta| < 2.0$) selected from the same dataset with the same trigger. The EM-like clusters are selected in a similar way to the photons except that no HITSINFO requirement is applied and that the cluster is required to have transverse and longitudinal shower profile $\chi^2 > 100$. These events are similar to those of the loose $\gamma+ \geq 2$ jets events and are expected to suffer from a similar $\not\!\!E_T$ mismeasurement.

As shown in the Fig. 1, the $\not\!\!E_T$ distributions of the two samples are in fact agree very well. In Fig. 9, the $\not\!\!E_T$ distributions of the QCD and $\gamma+ \geq 2$ jets samples are compared after the HITSINFO requirement. Again, the data distribution is reproduced well by the QCD distribution. Note that both data and QCD distributions with $\not\!\!E_T < 25$ GeV are obtained by convoluting the distributions of the entire samples before the HITSINFO by their respective fractions surviving the HITSINFO selection, where the fractions (shown in Fig. 8(a) and (b)) are determined using sub-samples processed with DØRECO version 12.20 or higher. Just like the data, all QCD background events with $\not\!\!E_T > 25$ GeV are picked and reprocessed with the good HITSINFO package. By normalizing the number of events with $\not\!\!E_T < 20$ GeV in the QCD sample to that in the $\gamma+ \geq 2$ jets sample, the number of QCD background events with $\not\!\!E_T > 25$ is found to be 316.4.

It is estimated that the EM-like clusters in $\sim 10\%$ of the selected QCD background events are due to photons. Increasing the χ^2 cut from 100 to 200 reduces the photon contribution

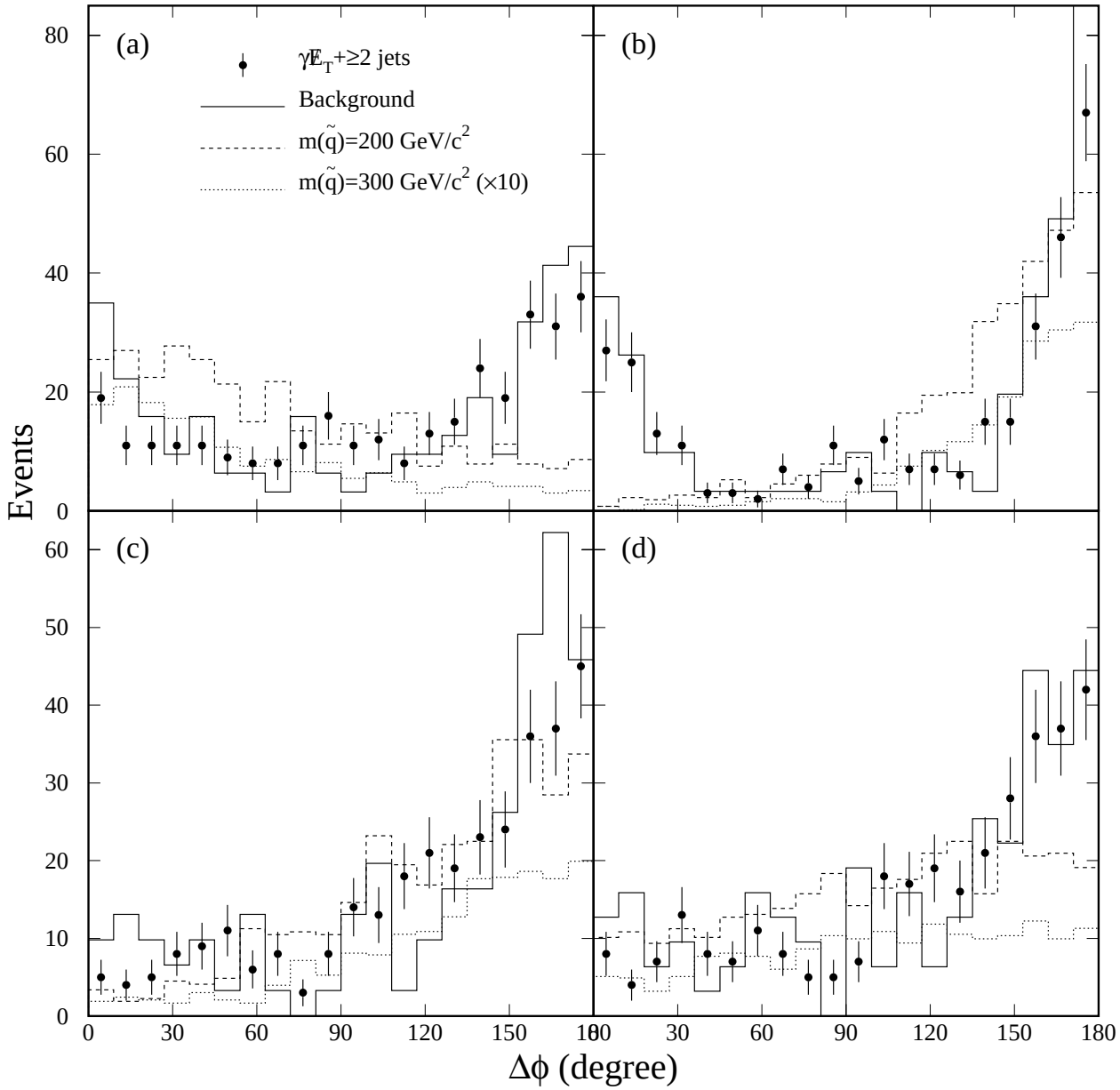

FIG. 7. Distributions of the $r-\phi$ opening angles beteween (a) the $\not\!\!E_T$ and the photon, (b) the $\not\!\!E_T$ and the leading jet, (c) the photon and the leading jet, and (d) the two leading jets for the $\gamma\not\!\!E_T+\geq 2$ jets and background events.

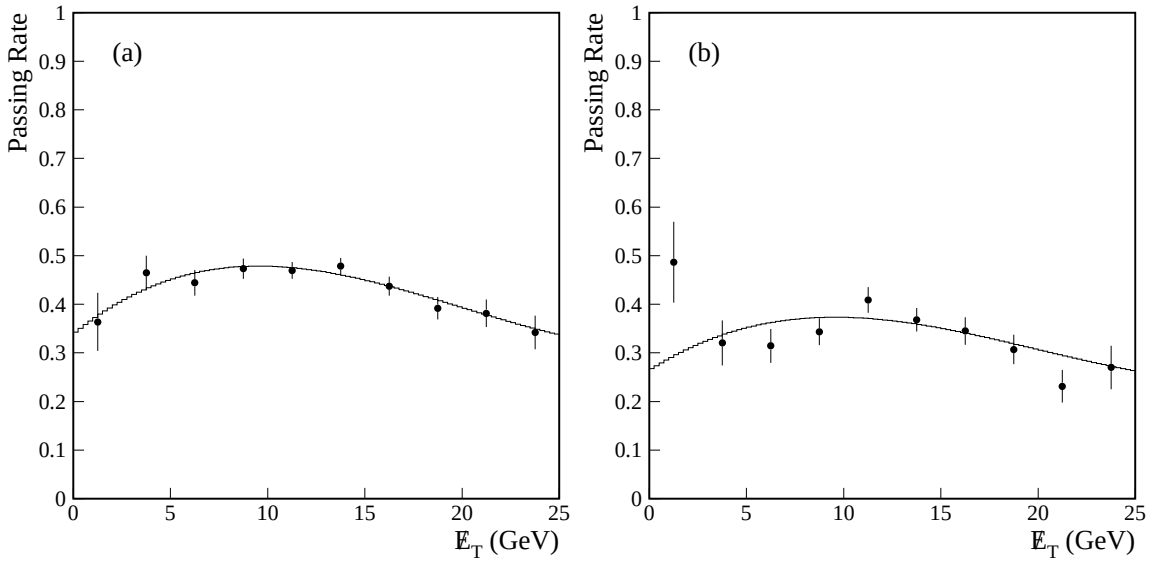

FIG. 8. The HITSINFO passing rate as a function of $\not\!\!E_T$ of the event for (a) loose $\gamma+ \geq 2$ jets events and (b) QCD background events. The rates are determined from sub-samples processed with the good HITSINFO package for $\not\!\!E_T$< 25 GeV. The histograms are fits to the same function with different overall normalization.

from 10% to 4% along with a 2% change in the estimated QCD background. We therefore assign a 2% systematic error to the estimation due to this uncertainty.

2. e+jets Background

To estimate the background contribution from the W+jets events, a sample of $W(\rightarrow e\nu)$+jets events with two or more jets ($E_T^j > 20$ GeV, $|\eta^j| < 2.0$) and $\not\!\!E_T$>25 GeV are selected from the same dataset and using the same trigger. We note that this sample includes events from all possible production sources, such as the direct W production in association with jets and indirect production of W from $t\bar{t}$ decays. Electrons selected from the identified EM clusters with matched tracks are required to satisfy the same E_T and η requirements as the photons. Taking into account the probability that an electron is misidentified as a photon, the number of background events from the e+jets production is estimated to be 4.2 in the $\gamma\not\!\!E_T+ \geq 2$ jets sample.

3. ν+jets Background

The ν+jets background due to W production is estimated using data and Monte Carlo samples of $W(\rightarrow e\nu)$ events, selected by requiring $\not\!\!E_T$> 25 GeV and three or more jets with $E_T^j > 20$ GeV and $|\eta^j| < 2.0$. The number of background events due to $W(\rightarrow \ell\nu) + 3$ jets production is approximately given by

$$N_W \sim 3 \times \left(\frac{N_{3j}}{N_{e+3j}}\right)_{MC} \times N_{e+3j}^{Data} \times \mathcal{P}_{j\rightarrow\gamma}$$

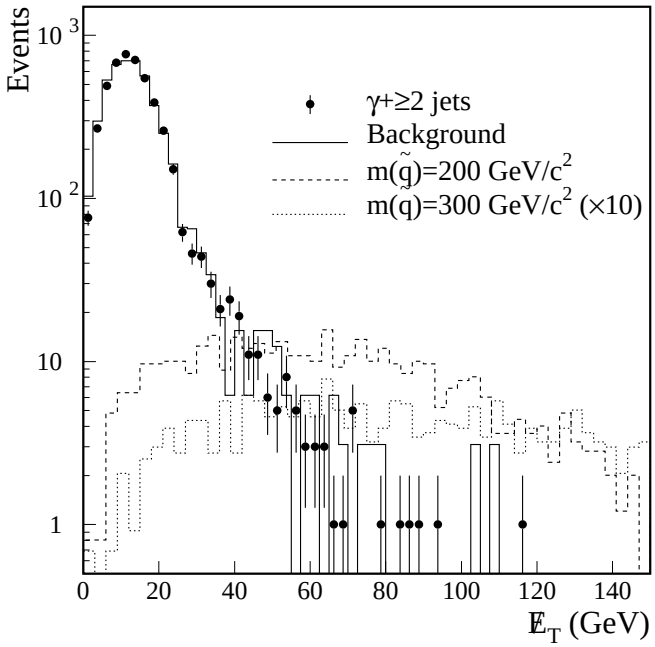

FIG. 9. The $\not\!\!E_T$ distribution (solid circle) of the events with one photon ($E_T^\gamma > 20$ GeV, $|\eta^\gamma| < 1.2$ or $1.5 < |\eta^\gamma| < 2.0$) and two or more jets ($E_T^j > 20$ GeV, $|\eta^j| < 2.0$). The expected $\not\!\!E_T$ distribution from the QCD background is shown in histogram. Note that the number of events with $\not\!\!E_T <$ 20 GeV in the background is normalized to that in the $\gamma+ \geq 2$ jets sample. Also showns are the distributions expected from supersymmetry for two different values of $m_{\tilde{q}}$.

where $\mathcal{P}_{j\to\gamma}$ is the probability of a jet faking a photon, N_{3j} is the number of jets in pseduorapidity range ($|\eta| < 1.2$ or $1.5 < |\eta| < 2.0$) of the photon identification in the selected W sample, N_{e+3j} is the same as N_{3j} but for the selected W sample with identified electrons, the factor 3 takes into account three lepton families. Again, electrons are selected from identified EM-clusters with matched tracks and are required to have $E_T^e > 20$ GeV and $|\eta^e| < 2.0$. The Monte Carlo factor $(\frac{N_{3j}}{N_{e+3j}})_{MC}$ corrects for the electron identification efficiency. The estimated number of background events from this source in the $\gamma\not\!\!E_T+ \geq 2$ jets sample is 1.7.

The other source of ν+jets background is from $Z(\to \nu\nu) + 3$ jets production. However, since the cross section of $Z(\to ee)$ is about 10% of that of $W(\to e\nu)$, the background due to the $Z(\to \nu\nu)+ \geq 3$ jets production is negligible.

C. Data and Background Comparions

The numbers of events observed and expected are summarized in Table III for the basic selection. Also listed in the tables are the breakdowns for number of events with three or more and four or more jets. Clearly, the non-QCD background is negligible. Within the statistics, the estimated number of background events agree with the number of observed events.

The expected background distributions are compared with the distributions of the

Number of jets	Events observed	Expected background QCD	e+jets	ν+jets	Total
$n \geq 2$	318	316.4±32.3	4.2±0.8	1.1±0.1	321.7±32.3
$n \geq 3$	70	69.2±15.3	0.7±0.1	0.2±0.1	70.1±15.3
$n \geq 4$	8	8.1±4.8	0.1±0.1	0.1±0.1	8.3±4.8

TABLE III. Number of observed $\gamma \not\!\!E_T + \geq n$ jets events together with the corresponding number of background events for $n = 2, 3, 4$.

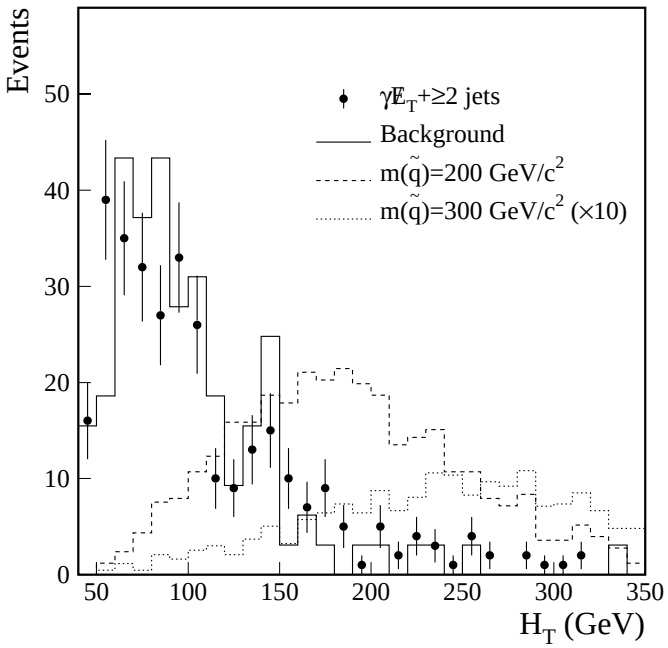

FIG. 10. The H_T distribution of the $\gamma \not\!\!E_T + \geq 2$ jets events. The expected distributions from the background events and the supersymmetry are also shown for comparisons.

$\gamma \not\!\!E_T + \geq 2$ jets events in Figs. 3-9. All background distributions agree well with the $\gamma \not\!\!E_T + \geq 2$ jets distributions. The E_T of the non-leading jets of the background events tends to be softer than that of the $\gamma \not\!\!E_T + \geq 2$ jets events. As shown in Table III, most of the 318 events are due to QCD $\gamma + \geq 2$ jets and multijet events with mismeasured $\not\!\!E_T$.

Questions have been raised whether the high $\not\!\!E_T$ and H_T tails are dominated by events with three or more jets. Fig. 11(a) and (b) show the $\not\!\!E_T$ and H_T distributions for $\gamma + 2$ jets and $\gamma + 3$ jets events for Run 1B. Evidently, $\gamma + 2$ jets events contribute significantly to the tails of both $\not\!\!E_T$ and H_T distributions.

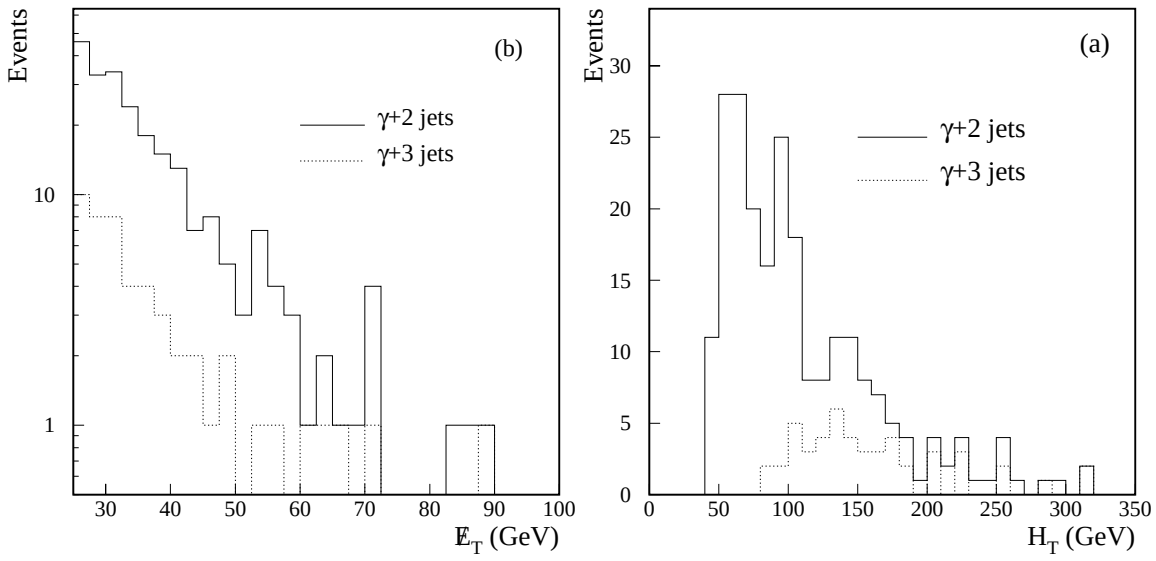

FIG. 11. The $\not\!\!E_T$ (a) and H_T (b) distributions of $\gamma + 2$jets and $\gamma + 3$jets events from Run 1B.

IV. LIMITS ON SUPERSYMMETRIC MODELS

In $p\bar{p}$ collisions, the production of squarks and gluinos in association with $\tilde{\chi}_2^0$ or with their subsequent decays to $\tilde{\chi}_2^0$ will yield events with a high E_T photon, multijets and large $\not\!\!E_T$. The process $p\bar{p} \to \tilde{\chi}_2^0 + X$ is used as a barometer for gauging sensitivity of this analysis to new physics. Though the direct $\tilde{\chi}_2^0$ production with other charginos and neutralinos will also yield $\gamma\not\!\!E_T$ events, the cross section for $\tilde{\chi}_2^0$ production is small (about 0.6 pb for the MSSM parameter values discussed below). Moreover, the number of jets is typically small and the jet E_T is usually soft in these events. The above $\gamma\not\!\!E_T + \geq n$ jets selection requirements have no sensitivity to this type of events which is, therefore, not considered here. To estimate the efficiency of the above $\gamma\not\!\!E_T + \geq n$ jets selection for $p\bar{p} \to \tilde{q}/\tilde{g} \to \tilde{\chi}_2^0 + X$ events, we simulate squark and gluino production using the SPYTHIA program [14], a supersymmetric extension of the PYTHIA 5.7 program [15]. The following processes $p\bar{p} \to \tilde{\chi}_i^{\pm}\tilde{q}, \tilde{\chi}_i^{\pm}\tilde{g}, \tilde{\chi}_j^0\tilde{q}, \tilde{\chi}_j^0\tilde{g}, \tilde{q}\tilde{q}, \tilde{q}\tilde{g}, \tilde{g}\tilde{g}$ are considered and the CTEQ3L parton distribution function [16] is used in the simulation. The details of the squark and gluino decays depend on values of the MSSM parameters. The charged sleptons ($\tilde{\ell}$) are assumed to have masses of 500 GeV/c^2 and the sneutrino ($\tilde{\nu}$) masses are fixed by the sum rule $m_{\tilde{\ell}}^2 = m_{\tilde{\nu}}^2 + M_W^2|\cos 2\beta|$, where M_W is the mass of the W boson. All stop productions (either direct or indirect) are ignored. The effect of a light stop ($\tilde{t}_1$) is discussed below. The MSSM parameters are set to $M_1 = M_2 = 60.0$ GeV, $\tan\beta = 2.0$ and $\mu = -40.0$ GeV. This set of parameter values gives $m_{\tilde{\chi}_1^0} = 33.5$ GeV/c^2, $m_{\tilde{\chi}_2^0} = 60.0$ GeV/c^2, $m_{\tilde{\chi}_3^0} = 91.5$ GeV/c^2, $m_{\tilde{\chi}_4^0} = 118.0$ GeV/c^2, $m_{\tilde{\chi}_1^{\pm}} = 63.8$ GeV/c^2, $m_{\tilde{\chi}_2^{\pm}} = 118.4$ GeV/c^2 and $\mathrm{Br}(\tilde{\chi}_2^0 \to \tilde{\chi}_1^0\gamma) = 100\%$. Events with $\tilde{\chi}_2^0$ in the final state are selected and run through a GEANT [17] based DØ detector simulation program and a trigger simulator. They are subjected to the DØRECO version 12.22. For simplicity, Monte Carlo events are generated for the following three squark/gluino mass scenarios: (1) equal squark and gluino mass ($m_{\tilde{q}} = m_{\tilde{g}}$), (2) light gluino and heavy squark ($m_{\tilde{g}} \ll m_{\tilde{q}}$=1 TeV) and (3) light squark and heavy gluino ($m_{\tilde{q}} \ll m_{\tilde{g}}$=1 TeV).

The expected distributions of several kinematic variables for $m_{\tilde{q}} = 200, 300$ GeV/c^2 are shown in Figs. 3-9,10. for the case $m_{\tilde{q}} = m_{\tilde{g}}$. In general, the photon and jet E_T, the $\not\!\!E_T$ and the H_T distributions expected from supersymmetry are considerablly harder than those of the $\gamma\not\!\!E_T+ \geq 2$ jets and background events. The numbers of events expected from supersymmetry passing the basic selection are 324 for $m_{\tilde{q}} = 200$ GeV/c^2 and 17.3 for $m_{\tilde{q}} = 300$ GeV/c^2.

To set cross section limit on the $p\bar{p} \to \tilde{g}/\tilde{q} \to \chi_2^0 + X$ production, we optimize the selection criteria (in a poor man's way!) for $\gamma\not\!\!E_T+ \geq 2$ jets and $\gamma\not\!\!E_T+ \geq 3$ jets events by varying $\not\!\!E_T$ and H_T requirements to maximize the $\frac{\epsilon}{\sigma_b}$ ratio for the $m_{\tilde{q}}(= m_{\tilde{g}}) = 300$ GeV/c^2 point **, where ϵ is the efficiency for supersymmetry and σ_b is the error on the estimated number of background events. It does not seem to make much difference whether the minimum number of jets requirement is two or three. The optimized cuts for $\not\!\!E_T$ and H_T are $\not\!\!E_T >$ 45 GeV and $H_T > 220$ GeV. With these cuts, five events are observed while 7.8 ± 5.7 events are expected from the background processes.

The efficiencies (ϵ) for supersymmetry are tabulated in Table IV for three scenarios of squark and gluino mass along with their respective fraction (ϵ_0) of generated events having $\tilde{\chi}_2^0$ in the final state. Though the and H_T cuts are optimized for $m_{\tilde{q}} = m_{\tilde{g}}$, these cuts also work well for the other two cases and are therefore kept the same. The errors are statistical only. In general, the efficiency ϵ increases as $m_{\tilde{q}/\tilde{g}}$ is increased. This is because the mass difference between $\tilde{\chi}_2^0$ and $\tilde{\chi}_1^0$ largely determines the photon E_T spectrum and the $m_{\tilde{q}}$ value determines H_T spectra to a large extent.

Parton level studies show that the efficiency varies within 4% for different choices of M_1, M_2, $\tan\beta$ and μ within the constraints $\mathrm{Br}(\tilde{\chi}_2^0 \to \tilde{\chi}_1^0\gamma) = 100\%$ and $m_{\tilde{\chi}_2^0} - m_{\tilde{\chi}_1^0} > 20$ GeV/c^2 ††. The variation is assigned as a systematic error in the efficiency. The total systematic error on the efficiency is estimated to be 9%, including 7% from photon identification, 4% from the choice of the supersymmetric parameter values and 3% from the jet energy scale uncertainty (estimated by applying HI/LOW CAFIX jet energy corrections to the Monte Carlo events).

We set a 95% confidence level (CL) upper limit on $\sigma(p\bar{p} \to \tilde{q}/\tilde{g} \to \tilde{\chi}_2^0 + X) \times \mathrm{Br}(\tilde{\chi}_2^0 \to \tilde{\chi}_1^0\gamma)$ ($\sigma \times$ Br) using a Bayesian approach [18] with a flat prior distribution for the signal cross section. The statistical and systematic uncertainties on the efficiency, the integrated luminosity, and the background estimation were included in the limit calculation with Gaussian prior distributions. The resulting upper limit as a function of squark/gluino mass is tabulated in Table V. The upper limit for the case $m_{\tilde{q}} = m_{\tilde{g}}$ is displayed in Fig. 12 and is compared with the theoretical cross sections, calculated using the CTEQ3L parton distribution function [16]. The hatched band represents the range of the theoretical cross section by varying the supersymmetric parameter values with the constraint $\mathrm{Br}(\tilde{\chi}_2^0 \to \tilde{\chi}_1^0\gamma) = 100\%$ and $m_{\tilde{\chi}_2^0} - m_{\tilde{\chi}_1^0} > 20$ GeV/c^2. The variation is about 20% for $m_{\tilde{q}} = 150$ GeV/c^2 and is

---

**An earlier version of this analysis using CAFIX 5.0 was optimized for every mass point. See appendix for details.

††This mass difference is imposed to ensure that photons from $\tilde{\chi}_2^0$ decays are reasonablly energetic, independent of the kinematic constraint of the CDF event.

$m_{\tilde{q}/\tilde{g}}$	Fractions/Efficiencies (%)					
	$m_{\tilde{q}} = m_{\tilde{g}}$		$m_{\tilde{g}} (\ll m_{\tilde{q}})$		$m_{\tilde{q}} (\ll m_{\tilde{g}})$	
GeV/c^2	ϵ_0	ϵ	ϵ_0	ϵ	ϵ_0	ϵ
150	66.2	1.7±0.3	69.1	1.5±0.3	60.0	2.3±0.4
200	62.3	7.9±0.6	59.6	5.3±0.6	53.8	9.5±0.9
250	59.6	14.8±0.8	49.7	13.6±1.1	55.4	14.8±1.1
300	56.1	21.5±1.0	43.1	19.0±1.3	55.4	22.1±1.2
350	51.8	22.8±1.1	39.3	23.5±1.5	52.7	26.6±1.4
400	46.7	23.5±1.1	33.3	22.7±1.6	54.3	25.8±1.3

TABLE IV. The efficiencies (ϵ) as functions of squark/gluino mass. ϵ_0 is the fraction of events generated with $\tilde{\chi}_2^0$ in the final state. The errors are statistical only. The estimated systematic error is 9%.

about 50% for $m_{\tilde{q}} = 300$ GeV/c^2. The intersection of our limit curve with the lower edge of the theory band is at $\sigma \times \mathrm{Br} = 0.38$ pb, leading to a lower limit on the mass of the squarks/gluinos of 311 GeV/c^2.

$m_{\tilde{q}/\tilde{g}}$	$\sigma \times$Br (pb)					
	$m_{\tilde{q}} (= m_{\tilde{g}})$		$m_{\tilde{g}} (\ll m_{\tilde{q}})$		$m_{\tilde{q}} (\ll m_{\tilde{g}})$	
GeV/c^2	Theory	Limit	Theory	Limit	Theory	Limit
150	83.4	5.3	24.1	6.3	8.51	4.3
200	12.1	1.1	3.48	1.6	1.59	0.90
250	2.37	0.57	0.51	0.63	0.43	0.58
300	0.53	0.39	0.12	0.44	0.12	0.38
350	0.13	0.37	0.02	0.37	0.03	0.32
400	0.04	0.36	0.005	0.37	0.008	0.32

TABLE V. Theoretical prediction and experimental 95% CL upper limit of $\sigma \times$ Br as functions of $m_{\tilde{q}/\tilde{g}}$ for $m_{\tilde{q}} = m_{\tilde{g}}$, $m_{\tilde{g}} \ll m_{\tilde{q}}$ and $m_{\tilde{q}} \ll m_{\tilde{g}}$. The theoretical predictions are calculated using the SPYTHIA program.

The effect of light sleptons on the squark and gluino decays is studied by varying the slepton mass ($m_{\tilde{\ell}}$) at parton level. The fraction of events containing at least one $\tilde{\chi}_2^0$ increases as the $m_{\tilde{\ell}}$ is decreased. When $m_{\tilde{\ell}}$ is varied from 500 GeV/c^2 to 80 GeV/c^2, the fraction increases about 23% for $m_{\tilde{q}} = 300$ GeV/c^2 and equal squark and gluino mass. Sleptons with mass below 80 GeV/c^2 have already excluded [20]. The increased $\tilde{\chi}_2^0$ production increases the mass limit by ~ 10 GeV/c^2.

A light stop ($\tilde{t}_1$) will also modify the squark and gluino decays and therefore affect the $\tilde{\chi}_2^0$ production. We investigate this effect by setting $m_{\tilde{t}_1} = 80$ GeV/c^2 which corresponds

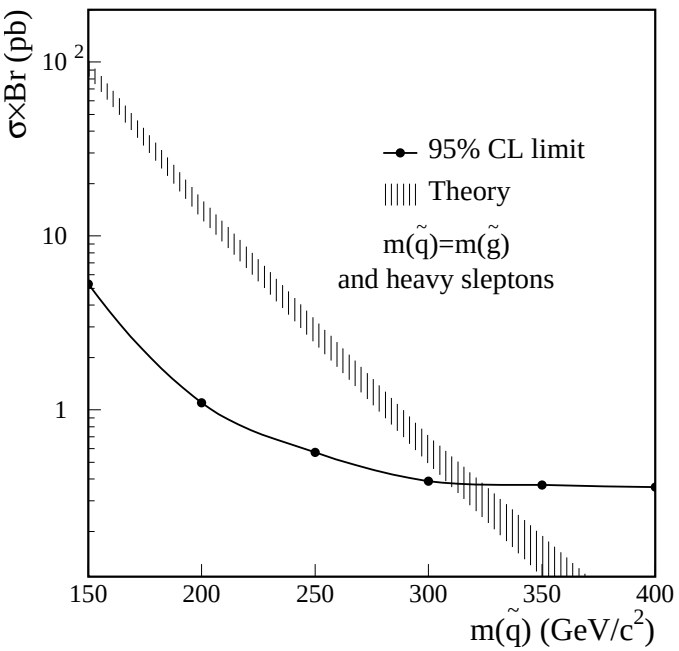

FIG. 12. The 95% CL upper limit on the $\sigma(p\bar{p} \to \tilde{q}/\tilde{g} \to \tilde{\chi}_2^0 + X) \times \mathrm{Br}(\tilde{\chi}_2^0 \to \chi_1^0\gamma)$ as a function of $m_{\tilde{q}/\tilde{g}}$ assuming an equal squark and gluino mass. The hatched band represents the range of the theoretical cross section for different sets of MSSM parameter values consistent with the constraint $\mathrm{Br}(\tilde{\chi}_2^0 \to \tilde{\chi}_1^0\gamma) = 100\%$ and $m_{\tilde{\chi}_2^0} - m_{\tilde{\chi}_1^0} > 20$ GeV/c^2.

to the lower mass limit from the LEP experiments [20]. A 15% reduction in $\tilde{\chi}_2^0$ production cross section is observed. This reduction lowers the limit on $m_{\tilde{q}}$ by ~ 6 GeV/c^2.

Following the same procedure, we obtain a low mass limit of gluinos (squarks) to be 239 GeV/c^2 (241 GeV/c^2) when squarks (gluinos) are heavy. Again, this limit varies $\sim$ 10 GeV/c^2 if $\tilde{t}_1$ or sleptons are light.

CDF collaboration carried out a similar analysis [19]. They examined a single point in the MSSM parameter space: $M_1 = M_2 = 60$ GeV, $\tan\beta = 1.0$ and $\mu = -40$ GeV. This set of parameter values is identical to what we used for the GEANT except for the $\tan\beta$ value. In addition, they assumed a light stop with mass $m_{\tilde{t}_1} = 60$ GeV/c^2 [‡‡]. They searched for events with a high E_T photon, a SVX tagged $b-$quark jet and large $\not\!\!E_T$ expected from the processes

$$p\bar{p} \to \tilde{q}/\tilde{g} \to \tilde{\chi}_i^{\pm}\tilde{\chi}_2^0 + n \text{ jets} \to (b\tilde{t}_1)(\tilde{\chi}_1^0\gamma) + n \text{ jets}$$

assuming $\mathrm{Br}(\tilde{t}_1 \to c\tilde{\chi}_1^0) = 100\%$ and $\mathrm{Br}(\tilde{\chi}_2^0 \to \tilde{\chi}_1^0\gamma) = 100\%$. From the analysis, they derived a mass limit of ~ 250 GeV/c^2 for equal squark/gluino mass and of ~ 190 GeV/c^2 when either squarks or gluinos are heavy. Despite of the very restrictive assumption for the stop sector of their analysis and their good $b-$tagging capability of the SVX, our limit is much stronger than theirs.

[‡‡] A light stop with its mass less than 67 GeV/c^2 has been excluded [20] by LEP experiments.

V. CONCLUSIONS

In summary, we have searched for excess of $\gamma \not\!\!E_T$ events with two or more jets in $p\bar{p}$ collisions at $\sqrt{s} = 1.8$ TeV for new physics. Such events are predicted in the minimal supersymmetric standard models. Though the physics background is small, we found that the instrumental background is large. For the selection criteria investigated in this note, we found that the number of observed $\gamma \not\!\!E_T + \geq n$ jets events agree well with that expected from background processes. Within the framework of the MSSM with the choices of the parameter values consistent with $\mathrm{Br}(\tilde{\chi}_2^0 \to \tilde{\chi}_1^0\gamma) = 100\%$ and $m_{\tilde{\chi}_2^0} - m_{\tilde{\chi}_1^0} > 20$ GeV/c^2, we obtain a 95% CL lower mass limit of 311 GeV/c^2 for the squarks and gluions assuming equal squark and gluino mass. This limit is stronger than that of CDF derived from the $\gamma b \not\!\!E_T$ analysis.

---

[1] For a review, see for example:
H. E. Haber and G. Kane, Phys. Rept. **117**, 75 (1985).

[2] S. Park, "*Search for New Phenomena in CDF*", 10th Topical Workshop on Proton-Antiproton Collider Physics, edited by R. Raja and J. Yoh, AIP Press, 1995.

[3] S. Ambrosanio *et al.*, Phys. Rev. Lett. **76**, 3498 (1996); Phys. Rev. D **55** 1372 (1997).

[4] S. Ambrosanio and B. Mele, Phys. Rev. D **55** 1399 (1997); Erratum-ibid. D **56** 3157 (1997).

[5] P. Fayet, Nucl. Phys. B**90**, 104 (1975);
A. Salam and J. Strathdee, Fortschr. Phys. **26**, 57 (1978).

[6] S. Chopra and J. Qian, "*Search for Supersymmetry as Predicted by Supersymmetric Models with A Light Gravitino*", DØnote #3141 (1997).

[7] J. Amundson *et al.*, "*Report of the Supersymmetry Theory Subgroup*", 1996 Snowmass summer studies, hep-ph/9609374.

[8] J. L. Lopez, D. V. Nanopoulos and A. Zichichi, "*Single-photon signals at LEP in supersymmetric models with a light gravitino*", hep-ph/9611437;
J. Gunion and C.-H. Chen, "*Maximizing hadron collider sensitivity to gauge-mediated supersymmetry breaking models*", hep-ph/9707302.

[9] DØ Collaboration, S. Abachi *et al.*, Nucl. Instrum. Methods **A338** (1994) 185.

[10] S. Chopra, U. Heintz and M. Narain, "*Comparison of Electron ID Efficiencies in Run 1A and 1B*", DØnote 2351.

[11] G. Landsberg, "*Search for Anomalous Couplings in the $Z(\nu\nu)\gamma$ Channel with Run Ia Data*", DØnote #3047.

[12] G. Landsberg, Ph.D. Dissertation, SUNY at Stony Brook (1994), unpublished.

[13] DØ Collaboration, S. Abachi *et al.*, Phys. Rev. Lett. 74 (1995) 2632; ibid Phys. Rev. D. **52** (1995) 4877.

[14] S. Mrenna, "*SPYTHIA, A Supersymmetric Extension of PYTHIA 5.7*", hep-ph/9609360.

[15] H.U. Bengtsson and T. Sjöstrand, Comp. Phys. Comm. **46** (1987) 43;
T. Sjöstrand, Comp. Phys. Comm. **82** (1994) 74.

[16] H. L. Lai *et al.*, Phys. Rev. **D51** (1995) 4763.

[17] R. Brun and F. Carminati, CERN Program Library Long Writeup W5013, 1993 (Unpublished).
[18] Particle Data Group, R. M. Barnett *et al.*, Phys. Rev. D **54**, 165 (1996);
J. Hobbs, the DØ limit program http://d0sgi0.fnal.gov/ hobbs/limit_calc.html;
I. Bertram *et al.*, "*A Recipe for the Construction of Confidence Limits*", DØnote #2775A.
[19] M. Gold, "*Search for Supersymmetry with the CDF Detector*", talk given at the XIIth Hadron Collider Physics Workshop, Jun 5-11, 1997, Stony Brook, New York.
[20] Reference to LEP limits on sleptons and stop...

Appendix: Summary of the Analysis with CAFIX 5.0

This analysis was done with CAFIX 5.0 earlier. The number of events observed and expected for the basic selection using CAFIX 5.0 are summarized in Table VI. To set cross section limit, the $\not\!\!E_T$ and H_T cuts were optimized to maximize the ϵ/σ_b ratio for every $m_{\tilde{q}} = m_{\tilde{g}}$ mass point. The optimized cuts for $\not\!\!E_T$ and H_T are tabulated in Table VII. The efficiencies for supersymmetry for these optimized cuts are tabulated in Table VIII and the resulting 95% CL upper limits on $\sigma \times Br$ are shown in Table IX. The lower mass limit is 311 GeV/c^2 for $m_{\tilde{q}} = m_{\tilde{g}}$, 233 GeV/c^2 for $m_{\tilde{q}} \gg m_{\tilde{g}}$ and 219 GeV/c^2 for $m_{\tilde{q}} \ll m_{\tilde{g}}$. The upper limit for the case $m_{\tilde{q}} = m_{\tilde{g}}$ is displayed in Fig. 13.

Number	Events	Expected background			
of jets	observed	QCD	e+jets	ν+jets	Total
$n \geq 2$	378	370.3±35.7	4.19±0.76	1.08±0.08	375.6±35.7
$n \geq 3$	74	74.9±16.3	0.70±0.14	0.24±0.04	75.8±16.2
$n \geq 4$	10	7.6±4.5	0.12±0.04	0.07±0.03	7.8±4.5

TABLE VI. Number of observed $\gamma\not\!\!E_T+ \geq n$ jets events together with the corresponding number of background events for $n = 2, 3, 4$.

$m_{\tilde{q}/\tilde{g}}$	$\not\!\!E_T$	H_T	Observed	Expected
(GeV/c^2)	(GeV)	(GeV)	$\gamma\not\!\!E_T+ \geq 2$ jets events	$\gamma\not\!\!E_T+ \geq 2$ jets events
150	>35	>100	60	74.7±16.7
200	>35	>100	60	74.7±16.7
250	>45	>150	13	15.1±7.7
300	>45	>220	5	8.1±5.8
350	>45	>220	5	8.1±5.8
400	>45	>220	5	8.1±5.8

TABLE VII. The optimized $\not\!\!E_T$ and H_T cuts for different values of $m_{\tilde{q}/\tilde{g}}$. Also shown are the numbers of observed and expected $\gamma\not\!\!E_T+ \geq 2$ jets events.

$m_{\tilde{q}/\tilde{g}}$	Fractions/Efficiencies (%)					
	$m_{\tilde{q}} = m_{\tilde{g}}$		$m_{\tilde{g}} (\ll m_{\tilde{q}})$		$m_{\tilde{q}} (\ll m_{\tilde{g}})$	
GeV/c^2	ϵ_0	ϵ	ϵ_0	ϵ	ϵ_0	ϵ
150	66.2	15.1±0.8	69.1	11.6±0.9	60.0	16.8±1.0
200	62.3	23.3±1.0	59.6	20.6±1.2	53.8	24.4±1.3
250	59.6	22.1±1.0	49.7	18.4±1.2	55.4	23.1±1.3
300	56.1	21.5±1.0	43.1	19.0±1.3	55.4	22.1±1.2
350	51.8	22.8±1.1	39.3	23.5±1.5	52.7	26.6±1.4
400	46.7	23.5±1.1	33.3	22.7±1.6	54.3	25.8±1.3

TABLE VIII. The efficiencies (ϵ) as functions of squark/gluino mass. ϵ_0 is the fraction of events generated with $\tilde{\chi}_2^0$ in the final state. The errors are statistical only. The estimated systematic error is 9%.

$m_{\tilde{q}/\tilde{g}}$	$\sigma \times$Br (pb)					
	$m_{\tilde{q}} (= m_{\tilde{g}})$		$m_{\tilde{g}} (\ll m_{\tilde{q}})$		$m_{\tilde{q}} (\ll m_{\tilde{g}})$	
GeV/c^2	Theory	Limit	Theory	Limit	Theory	Limit
150	83.4	2.0	24.1	2.6	8.51	1.8
200	12.1	1.3	3.48	1.4	1.59	1.3
250	2.37	0.67	0.51	0.81	0.43	0.64
300	0.53	0.39	0.12	0.44	0.12	0.38
350	0.13	0.37	0.02	0.37	0.03	0.32
400	0.04	0.36	0.005	0.37	0.008	0.32

TABLE IX. Theoretical prediction and experimental 95% CL upper limit of $\sigma \times$ Br as functions of $m_{\tilde{q}/\tilde{g}}$ for $m_{\tilde{q}} = m_{\tilde{g}}$, $m_{\tilde{g}} \ll m_{\tilde{q}}$ and $m_{\tilde{q}} \ll m_{\tilde{g}}$. The theoretical predictions are calculated using the SPYTHIA program.

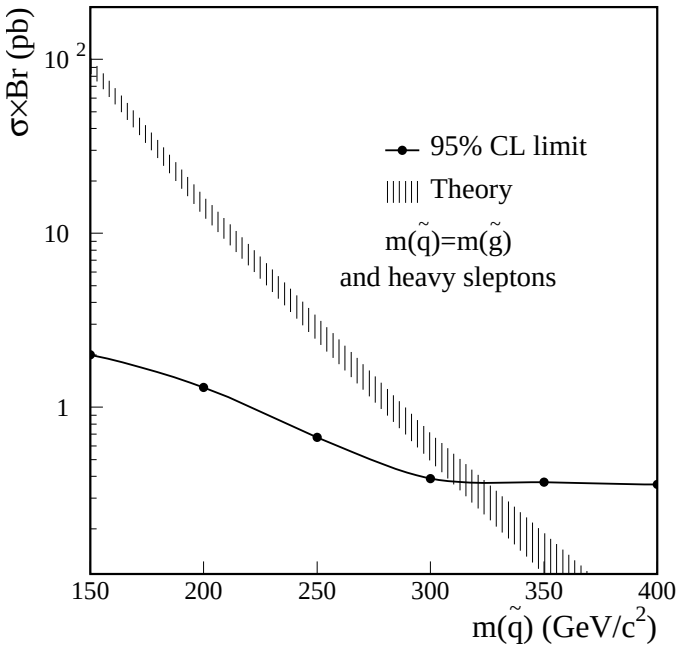

FIG. 13. The 95% CL upper limit on the $\sigma(p\bar{p} \to \tilde{q}/\tilde{g} \to \tilde{\chi}_2^0 + X) \times \mathrm{Br}(\tilde{\chi}_2^0 \to \chi_1^0\gamma)$ as a function of $m_{\tilde{q}/\tilde{g}}$ assuming an equal squark and gluino mass. The hatched band represents the range of the theoretical cross section for different sets of MSSM parameter values consistent with the constraint $\mathrm{Br}(\tilde{\chi}_2^0 \to \tilde{\chi}_1^0\gamma) = 100\%$ and $m_{\tilde{\chi}_2^0} - m_{\tilde{\chi}_1^0} > 20$ GeV/c^2.